



Imaging findings in a case of primary intraosseous carcinoma arising from a mandibular cyst

Yukiko Kami¹ · Toru Chikui¹ · Shinsuke Fujii^{2,3} · Tatsufumi Fujimoto^{2,4} · Wataru Kumamaru⁴ · Kana Hasegawa² · Koji Nakamatsu⁵ · Kazutoshi Okamura¹ · Misa Yasaka¹ · Tamotsu Kiyoshima² · Kazunori Yoshiura⁶

Received: 11 June 2024 / Accepted: 10 November 2024 / Published online: 23 November 2024
© The Author(s) under exclusive licence to Japanese Society for Oral and Maxillofacial Radiology 2024

Abstract

Primary intraosseous carcinoma not otherwise specified (PIOC NOS) is a rare tumor assumed to arise from the epithelium, such as odontogenic cysts or benign tumors. Its clinical and imaging diagnoses are often challenging, especially in the early stages, as it mimics jaw cysts and benign tumors, and no specific findings have been identified. This report presents the case of a 66-year-old male patient with mandibular PIOC, highlighting the imaging findings over time. Magnetic resonance imaging (MRI) before symptom onset showed a cystic lesion in the right mandible with a soft tissue component. Both the fluid component and soft tissue exhibited low apparent diffusion coefficient values ($1.0 \times 10^{-3} \text{ mm}^2/\text{s}$ and $1.3 \times 10^{-3} \text{ mm}^2/\text{s}$, respectively). Subsequent MRI approximately 5 months later during symptom onset showed a slight increase in the soft tissue component. Based on the clinical and imaging findings, ameloblastoma was suspected, prompting a biopsy for confirmation. However, the histopathological findings showed squamous cell carcinoma (SCC). MRI performed approximately 1 month later exhibited significant tumor growth and extension beyond the jawbone, consistent with a malignant tumor. Histopathological examination identified areas with a basal layer in a palisading arrangement, indicating a pre-existing odontogenic cyst, and showed a transition from epithelial dysplasia to SCC. In addition, carcinoma cell invasion and proliferation into the cyst were observed. Based on these findings, PIOC of the right mandible was determined to be the definitive diagnosis.

Keywords Primary intraosseous carcinoma · Mandible · Cyst · Imaging findings · Magnetic resonance imaging

Introduction

Primary intraosseous carcinoma not otherwise specified (PIOC NOS) is a rare malignant tumor, accounting for 1–2% of all oral cancers [1, 2]. The 2022 World Health Organization (WHO) classification defines PIOC as a central jaw carcinoma that cannot be categorized as any other type of carcinoma and derives from odontogenic cyst, rests of odontogenic epithelium, the reduced enamel epithelium surrounding impacted teeth, or other benign precursors [3]. Diagnosing PIOC, particularly in the early stages, poses a significant challenge because clinical and imaging findings often mimic those of jawbone cysts and benign odontogenic tumors such as residual/radicular cysts, dentigerous cysts, odontogenic keratocysts, and ameloblastomas. Therefore, they are often identified by histopathology and, in some cases, have already infiltrated a large area by the time they are diagnosed [1, 4–8]. This report presents a longitudinal review of imaging findings from a case of mandibular PIOC,

✉ Yukiko Kami
kami@rad.dent.kyushu-u.ac.jp

¹ Department of Oral and Maxillofacial Radiology, Faculty of Dental Science, Kyushu University, 3-1-1, Maidashi, Higashi-ku, Fukuoka 812-8582, Japan

² Laboratory of Oral Pathology, Division of Maxillofacial Diagnostic and Surgical Sciences, Faculty of Dental Science, Kyushu University, Fukuoka, Japan

³ Dento-Craniofacial Development and Regeneration Research Center, Faculty of Dental Science, Kyushu University, Fukuoka, Japan

⁴ Section of Oral and Maxillofacial Surgery, Division of Maxillofacial Diagnostic and Surgical Sciences, Faculty of Dental Science, Kyushu University, Fukuoka, Japan

⁵ Department of Dentistry and Oral Surgery, Iizuka Hospital, Fukuoka, Japan

⁶ Fukuoka, Japan

highlighting the changes in the lesion before symptom onset, after symptom onset, and after biopsy.

Case report

A 66-year-old male patient presented to a local dentist in February 2023 with right-sided mandibular pain, oral vestibule swelling, and gingival sulcus effusion upon finger pressure. Panoramic radiography showed radiolucency in the mandible, prompting referral to the Oral Surgery Department of a general hospital for further evaluation. Based on the clinical findings of normal mucosa, imaging findings of cone-beam computed tomography (CBCT) and magnetic resonance imaging (MRI), ameloblastoma was suspected. On March 11, 2023, the patient underwent fenestration with mandibular anterior teeth extraction and biopsy, and was histopathologically diagnosed with squamous cell carcinoma (SCC). Based on these findings, the patient was referred to the Oral Surgery Department of our university hospital on March 20, 2023. Extraoral examination presented swelling, redness, and tenderness in the right submandibular region. No paresthesia was present in the lower lip or the submental region. No swelling, tenderness, or adhesion was noted in the submandibular lymph nodes, and the patient exhibited maximal mouth opening of approximately three fingerbreadths. Intraoral examination presented gauze contamination on the fenestration site and a mild bulge in the buccal cortical bone. Several teeth in the right mandible were missing, and according to the patient, one of them had been extracted more than 20 years ago due to a cyst. The patient's medical history included hypertension and a previous lipoma excision surgery in the right posterior neck in November 2022.

The detailed imaging findings over time are as follows: The chronological timeline of the image acquisition is shown in Fig. 1. With the patient's history of removal of lipoma in the right posterior neck, MR images from that time acquired at one general hospital on October 17, 2022, were obtained, showing a portion of the current lesion (Fig. 2). A single cystic lesion extending from the

anterior mandibular region to the right premolar region was observed, which had a slightly higher signal intensity than the muscle on T1-weighted images (T1-WI). T2-weighted images (T2-WI) showed an overall high signal intensity with interspersed heterogeneous low-signal areas. Gadolinium-enhanced T1-weighted images (Gd T1-WI) showed areas within the lesion suggestive of soft tissue and fluid components. The apparent diffusion coefficient (ADC) values were approximately $1.0 \times 10^{-3} \text{ mm}^2/\text{s}$ for the fluid component and $1.3 \times 10^{-3} \text{ mm}^2/\text{s}$ in the vicinity of the soft tissue component.

Figure 3 presents the images obtained at the referred general hospital on March 1, 2023. Panoramic radiography exhibited a unifocal radiolucency extending from the anterior mandibular region to the right premolar region (Fig. 3a). The lesion overlapped with the root apex of the anterior mandibular teeth and was partially close to the alveolar apex. Its lower portion was located near the inferior margin of the mandible. CBCT showed mild expansion, thinning, and loss of buccolingual cortical bone due to the lesion (Fig. 3b). The mandibular canal was compressed to the buccal side. Mild osteosclerosis was observed around the lesion. MRI showed a slight increase in soft tissue components within the cystic lesion (Fig. 3c). Diffusion-weighted imaging was not performed. Given these findings, ameloblastoma was suspected, prompting the performance of fenestration with mandibular anterior teeth extraction and biopsy on March 11, 2023. Figure 4 shows histopathological images of the biopsy, which consists of dense and loose fibrous connective tissues and inflamed granulation tissue with moderate infiltration of lympho-plasmacytes, multinucleated giant cells associated with cholesterol clefts, and foamy macrophages partially lined by squamous epithelium (Fig. 4a). Histopathological findings showed a transition from the epithelial dysplastic changes such as multilayered basaloid cells to a proliferation of atypical squamous cells in the irregular- and bulky-elongated rete ridges, indicating SCC (Fig. 4b), and an invasive growth of SCC cells into the sub-epithelial layer (Fig. 4c). The lesion was histopathologically diagnosed as an SCC.

Figure 5 shows the images obtained at our university hospital between March 29 and 31, 2023. The soft tissue was

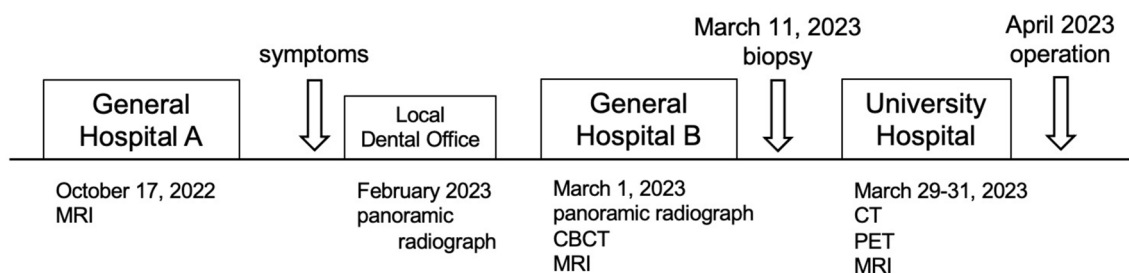


Fig. 1 The chronological timeline of image acquisition. *MRI* magnetic resonance imaging, *CBCT* cone-beam computed tomography, *CT* computed tomography, *PET* positron emission tomography

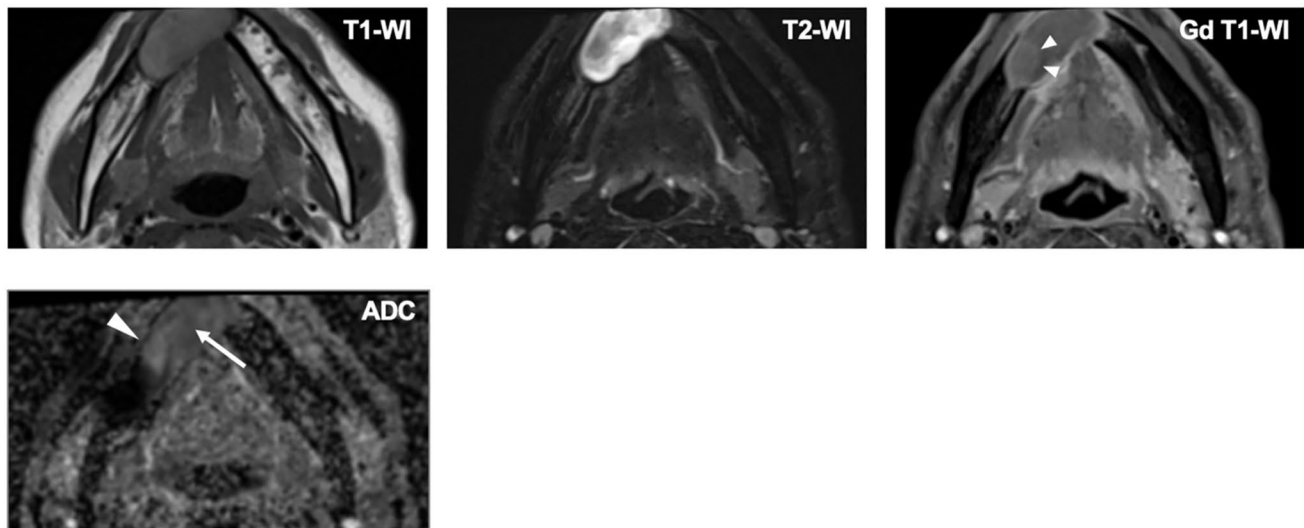


Fig. 2 MRI performed on October 17, 2022, showing a cystic lesion in the right mandible. T1-WI showed slightly higher signal intensity than the muscle. T2-WI showed an overall higher signal intensity with interspersed low-signal areas. Gd T1-WI showed a soft

tissue-like component within a slightly higher signal fluid component (arrowheads). ADC values were approximately $1.0 \times 10^{-3} \text{ mm}^2/\text{s}$ for the fluid component (arrow) and $1.3 \times 10^{-3} \text{ mm}^2/\text{s}$ in the vicinity of the soft tissue component (arrowhead)

rapidly enlarged, spreading outward from the lingual side of the jawbone to the submandibular and skin surfaces, and partial necrosis was observed. The time–signal intensity curve demonstrated rapid enhancement with a low washout curve. ADC values within the soft tissue compartment and near the fluid compartment were approximately $1.0 \times 10^{-3} \text{ mm}^2/\text{s}$ and $0.8 \times 10^{-3} \text{ mm}^2/\text{s}$, respectively. The maximum standardized uptake value of F-18 fluorodeoxyglucose positron emission tomography/computed tomography was 31.3. The imaging diagnosis was a malignant tumor on the right side of the mandible (T4aN0M0). In April 2023, the patient underwent a right segmental mandibulectomy with right modified radical neck dissection and left selective neck dissection. The right mandible was reconstructed using a plate and an anterolateral thigh flap. Figure 6 shows the histopathological images of the excised specimens. Certain areas in the epithelium showed characteristic basal cells, which were palisaded, ranged from cuboidal to columnar, and partially showed reverse nuclear polarity, suggesting pre-existing odontogenic cystic epithelium (Fig. 6a, b(A)). A transition from epithelial dysplasia to SCC (carcinoma in situ) (Fig. 6a, b(B)) and tumor cell invasion and proliferation into the cystic wall were observed (Fig. 6a,

b(C, D). No lymph node metastasis was observed. The definitive diagnosis was a PIOC arising from a cyst in the right mandible.

Discussion

According to the 2022 WHO classification, PIOC is defined as a central jaw carcinoma that cannot be categorized as any other type of carcinoma and derives from odontogenic cyst, rests of odontogenic epithelium, the reduced enamel epithelium surrounding impacted teeth, or other benign precursors. An intraosseous origin must be established for the diagnosis, excluding extension of gingival or alveolar SCC or antral carcinoma into the jaws. Metastases must be excluded [3]. In this case, PIOC was definitively diagnosed based on histopathological findings of a basal layer with cell palisading arrangement suggestive of a pre-existing odontogenic cyst, and a transition from epithelial dysplasia to SCC. PIOC are often difficult to diagnose based on clinical and imaging findings, especially in their early stages, because they mimic jawbone cysts and benign odontogenic tumors [4–8]. In this

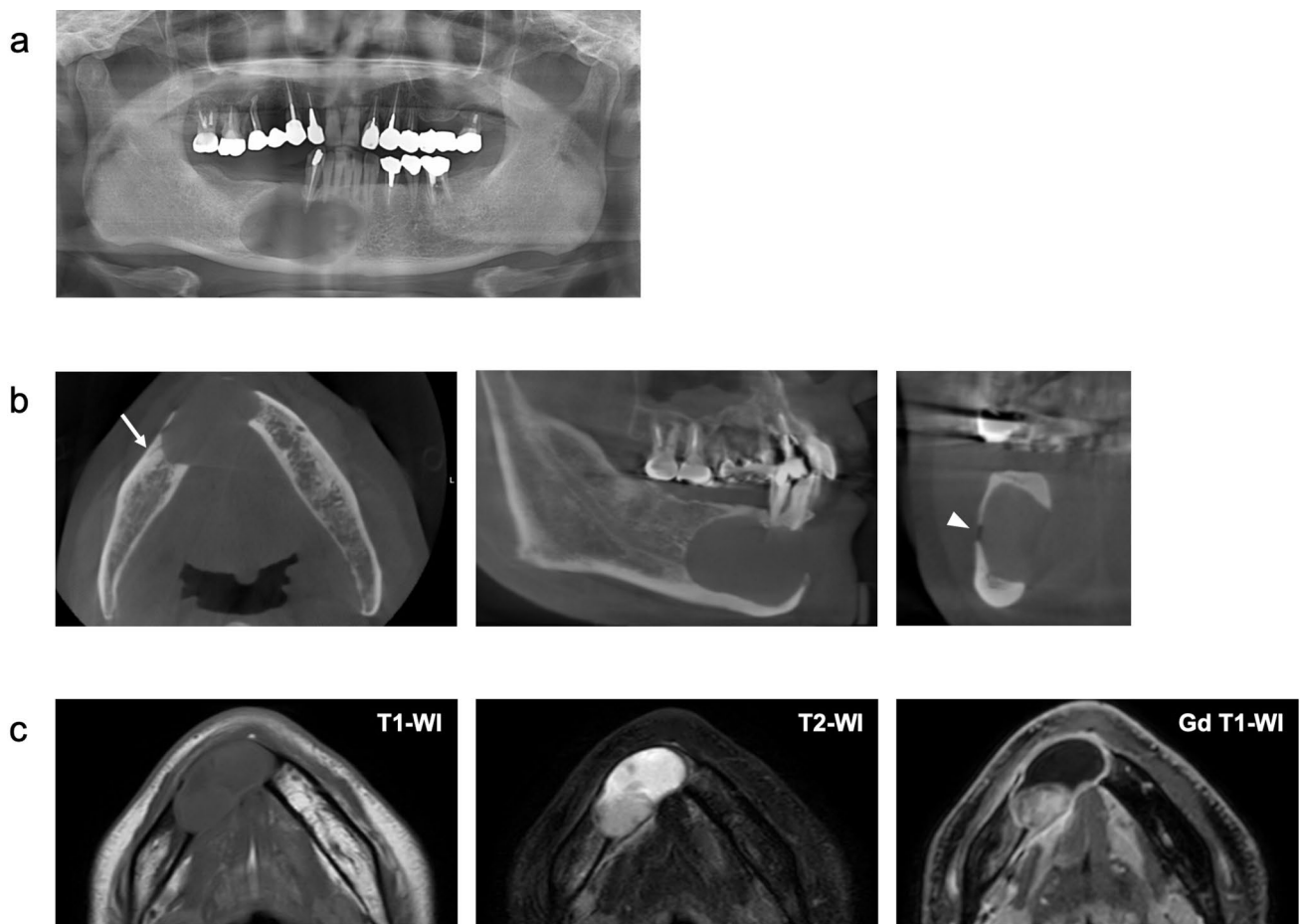


Fig. 3 Panoramic radiography (a), CBCT (b), and MRI (c) performed on March 1, 2023. Panoramic radiography exhibited a unifocal, radiolucent lesion in the right mandible. CBCT showed an expansive lesion compressing the mandibular canal toward the buccal side

(arrowhead) and mild osteosclerosis around the lesion (arrow). MRI showed a slight increase in soft tissue components within the cystic lesion

study, the mandibular PIOC was retrospectively evaluated over time using 3 dimensional (3D) images acquired at three different time points (Fig. 1). Although images were obtained at different institutions, to our knowledge, there are no reports on changes in PIOC over time with 3D imaging modalities such as CT or MRI.

The first images of this case were incidentally obtained prior to symptom onset (Fig. 2). MRI T1-WI showed a slightly higher signal intensity than the muscle; T2-WI showed low-signal areas within the high-signal regions, and Gd T1-WI showed a slightly higher signal intensity in areas suspected to be the fluid component. These findings indicate that the fluid component may have been present for a long period and concentrated; it could be a highly viscous

matrix containing proteins or other substances, or it could also contain necrotic cells or keratinization within the fluid component. Retrospectively observed, Gd T1-WI showed an area that appeared to be a soft tissue component. Both the fluid and soft tissue component areas exhibited lower ADC values, approximately $1.0 \times 10^{-3} \text{ mm}^2/\text{s}$ for the area of the fluid component and approximately $1.3 \times 10^{-3} \text{ mm}^2/\text{s}$ near the soft tissue component, which did not appear to be typical values reported in benign odontogenic tumors such as ameloblastoma. According to Sumi et al. [9], the ADC values of non-enhancing lesions and solid lesions in ameloblastomas were $2.48 \pm 0.20 \times 10^{-3} \text{ mm}^2/\text{s}$ and $1.39 \pm 0.16 \times 10^{-3} \text{ mm}^2/\text{s}$, respectively. Approximately 5 months later, MRI performed after symptom onset exhibited slight enlargement

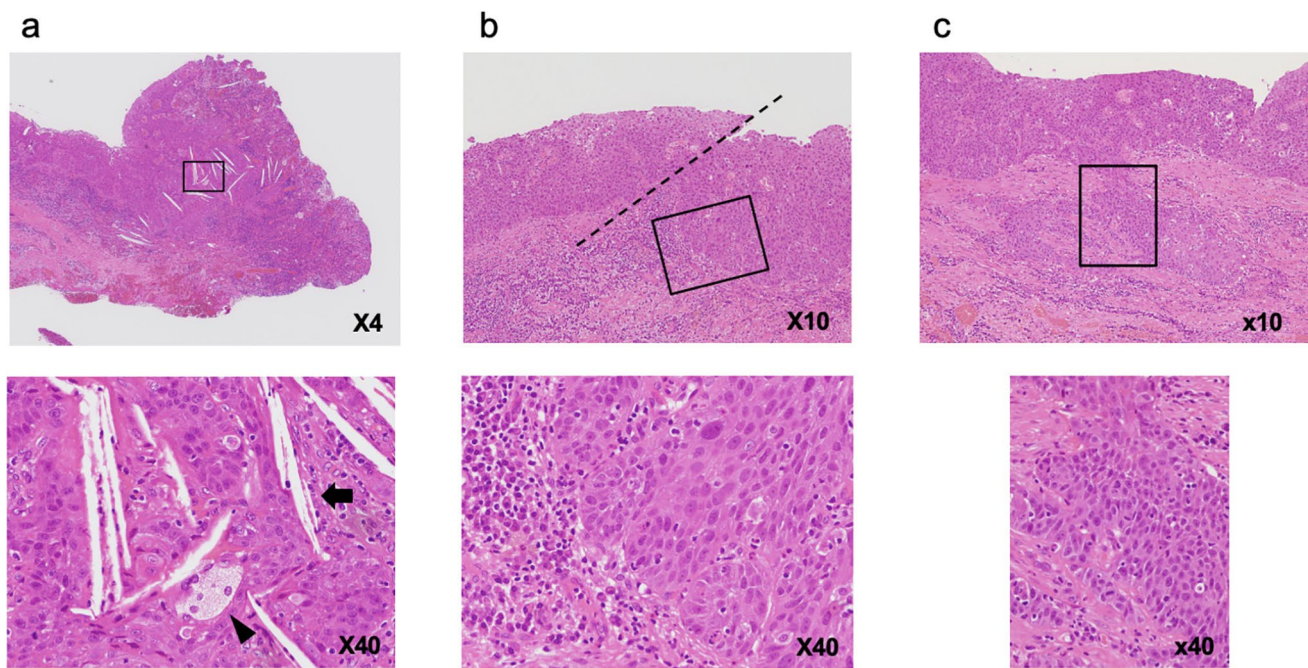


Fig. 4 Histopathological images of biopsy specimens. The solid boxes (**a**, **b**, and **c**) are enlarged in the lower panels of images **a**, **b**, and **c**, respectively. Certain epithelial areas showed inflammation with cholesterol clefts (**a**: arrow) and foamy macrophages (**a**: arrowhead).

A transition from moderate epithelial dysplasia (**b**: left side of the dotted line) to SCC (**b**: right side of the dotted line) and invasion of SCC into the sub-epithelial layer (**c**) were observed in the lesion

and clarification of the soft tissue component (Fig. 3). The fluid component showed a high signal on T2-WI and was not contrasted with the Gd T1-WI. Although potential device-related imaging variations cannot be completely excluded, the concentrated fluid component might have leaked out, which would explain the observed gingival sulcus effusion, and was replaced by a new fluid component. Images obtained at our university hospital approximately 20 days after fenestration and biopsy showed significant tumor growth and extension beyond the jawbone (Fig. 5), which was consistent with malignancy.

Naruse et al. [2] reported that pre-diagnostic interventions were significantly associated with poor 2-year relapse-free survival and overall survival rates in PIOC. Conversely, patients who did not receive treatment prior to diagnosis exhibited no locoregional recurrence. In our case, it is possible that the intervention of fenestration with teeth extraction may have caused the rapid growth of the tumor [2, 10]. Preoperative diagnosis is ideal, but accurate PIOC diagnosis based on imaging and clinical findings can be challenging. If something to point out, the ADC values of the soft tissue and fluid components were not consistent with those of

normal benign tumors in this case. Long-standing chronic inflammation has been proposed as the principal predisposing factor for malignant transformation in the epithelial lining of cysts; however, this cannot be substantiated [11]. In this case, CBCT showed slight osteosclerosis around the lesion, and the biopsy results showed signs of inflammation, such as cholesterol clefts and macrophages, but the inflammatory findings were similar to those seen in common jawbone cysts, such as radicular cysts. Nevertheless, PIOC diagnosis and minimal pre-diagnostic interventions should be considered in cases where imaging findings are inconsistent with those of benign tumors or when signs are suggestive of chronic inflammation.

Residual/radicular cysts are the most common origin of PIOC (60%), followed by dentigerous cysts and odontogenic keratocysts [1]. The patient remembered tooth extraction due to a right mandibular cyst more than 20 years ago, but no confirmatory images or medical records were available to prove this. Assuming that the cause of the extraction was an odontogenic cyst, the lesion most likely originated from a residual/radicular cyst. Based on the current findings, careful image evaluation should

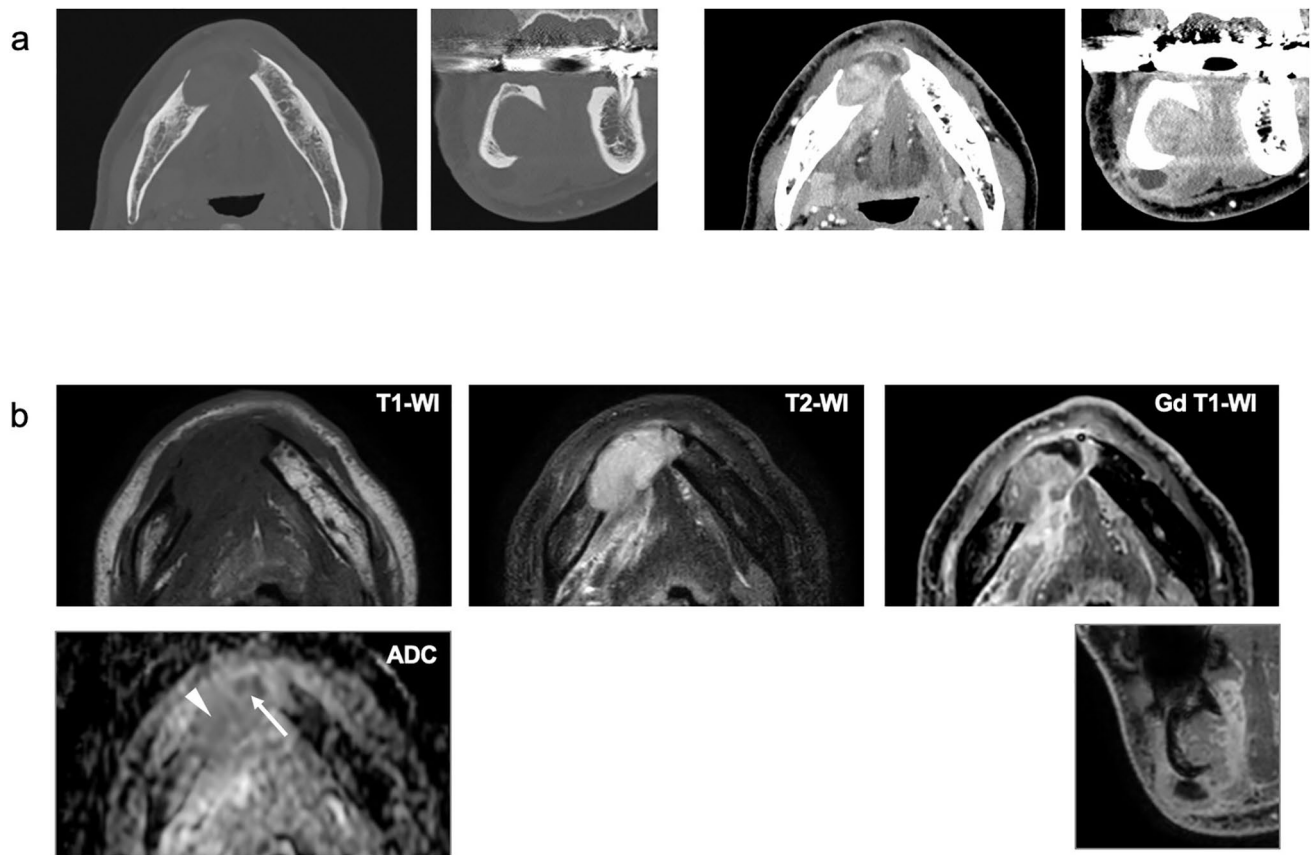


Fig. 5 CT (a) acquired on March 29, 2023, and MRI (b) on March 31, 2023. The lesion was almost entirely occupied by soft tissue, spread linguallly from the jawbone to the submandibular and skin surfaces, and partial necrosis was observed. ADC values within the

soft tissue compartment (arrowhead) and near the fluid compartment (arrow) were approximately $1.0 \times 10^{-3} \text{ mm}^2/\text{s}$ and $0.8 \times 10^{-3} \text{ mm}^2/\text{s}$, respectively

be performed even in cystic cases in which malignancy is not suspected clinically. At a minimum, if changes are observed within the cystic cavity, pathological examination, including biopsy, is recommended.

In conclusion, this report presents the imaging findings of PIOC in the mandible over time. In this case, soft tissue was found within a cystic lesion in the mandible that gradually

increased in size. Both the soft tissue and fluid components within the lesion showed lower ADC values than those of common cysts or benign odontogenic tumors. The soft tissue suggested malignancy, and the fluid component had the impression of a liquid that had been present for a long period and concentrated. It could be a highly viscous matrix

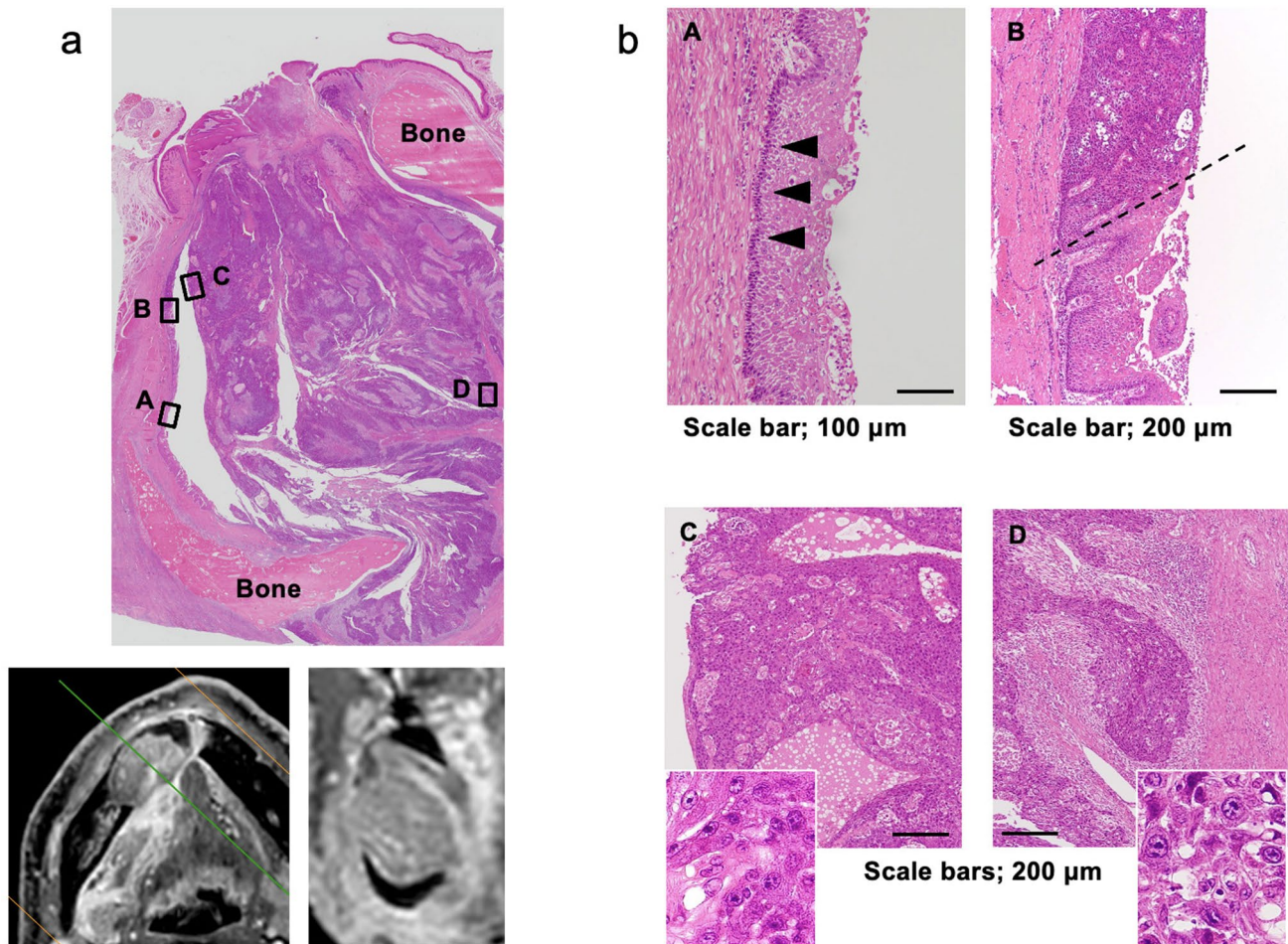


Fig. 6 Histopathological images of the excised specimens. MRI shows the location of the pathological section (a). Magnified images of areas A–D are shown in (b). Certain areas in the epithelium showed characteristic basal cells, which were palisaded, ranged from cuboidal to columnar, and partially showed reverse nuclear polarity,

suggesting pre-existing odontogenic cystic epithelium (A), and transition from epithelial dysplasia to SCC (carcinoma in situ) (B: above the dotted line). Tumor cell invasion and proliferation into the cystic wall were observed in areas C and D. The solid boxes in areas C and D are enlarged in lower panels

containing proteins or other substances, or it could contain necrotic cells or keratinization. Accumulation of the findings of changes over time, including imaging findings, in many PIOC cases can contribute to providing a correct diagnosis and appropriate treatment for PIOC.

Funding This study was supported by JSPS KAKENHI (grant number JP22K10174).

Data availability No new data were created or analyzed in this study. Data sharing is not applicable to this article.

Declarations

Conflict of interest All authors declare that they have no conflict of interest.

Ethical approval All procedures followed were in accordance with the ethical standards of the responsible committee on human experimentation (institutional and national) and with the Helsinki Declaration of 1975, as revised in 2008 (5). At our institution, ethical review is waived for case reports, although informed consent must be obtained from the patient.

Informed consent Informed consent was obtained from the patient for being included in the study.

References

1. Bodner L, Manor E, Shear M, van der Waal I. Primary intraosseous squamous cell carcinoma arising in an odontogenic cyst: a clinicopathologic analysis of 116 reported cases. *J Oral Pathol Med.* 2011;40:733–8. <https://doi.org/10.1111/j.1600-0714.2011.01058.x>.

2. Naruse T, Yanamoto S, Sakamoto Y, Ikeda T, Yamada SI, Umeda M. Clinicopathological study of primary intraosseous squamous cell carcinoma of the jaw and a review of the literature. *J Oral Maxillofac Surg.* 2016;74:2420–7. <https://doi.org/10.1016/j.joms.2016.05.006>.
3. Koutlas IG, Sloan P. WHO classification of tumours 5th edition, head and neck tumours. Geneva: WHO Classification of Tumours Editorial Board, International Agency for Research on Cancer, World Health Organization; 2024. p. 373–4.
4. Abdelkarim AZ, Elzayat AM, Syed AZ, Lozanoff S. Delayed diagnosis of a primary intraosseous squamous cell carcinoma: a case report. *Imaging Sci Dent.* 2019;49:71–7. <https://doi.org/10.5624/isd.2019.49.1.71>.
5. Marchal A, Gérard É, Curien R, Bourgeois G. Primary intraosseous carcinoma arising in dentigerous cyst: case report. *Int J Surg Case Rep.* 2020;76:530–3. <https://doi.org/10.1016/j.ijscr.2020.10.059>.
6. Takahashi H, Takaku Y, Kozakai A, Otsuru H, Murata Y, Myers MW. Primary intraosseous squamous cell carcinoma arising from a dentigerous cyst of the maxillary wisdom tooth. *Case Rep Oncol.* 2020;13:611–6. <https://doi.org/10.1159/000507478>.
7. de Moraes EF, Carlan LM, de Farias Moraes HG, Pinheiro JC, Martins HDD, Barboza CAG, et al. Primary intraosseous squamous cell carcinoma involving the jaw bones: a systematic review and update. *Head Neck Pathol.* 2021;15:608–16. <https://doi.org/10.1007/s12105-020-01234-z>.
8. Al-Harbaee A, Mair M, Rajaram K, Baker A, Da Forno P. Primary intraosseous squamous cell carcinoma: a rare malignancy of the mandible. *Adv Oral Maxillofac Surg.* 2021;2:100063. <https://doi.org/10.1016/j.adoms.2021.100063>.
9. Sumi M, Ichikawa Y, Katayama I, Tashiro S, Nakamura T. Diffusion-weighted MR imaging of ameloblastomas and keratocystic odontogenic tumors: differentiation by apparent diffusion coefficients of cystic lesions. *AJNR Am J Neuroradiol.* 2008;29:1897–901. <https://doi.org/10.3174/ajnr.A1266>.
10. Nomura T, Monobe H, Tamaruya N, Kishishita S, Saito K, Miyamoto R, Nakao K. Primary intraosseous squamous cell carcinoma of the jaw: two new cases and review of the literature. *Eur Arch Otorhinolaryngol.* 2013;270(1):375–9. <https://doi.org/10.1007/s00405-012-2235-9>.
11. Schwimmer AM, Aydin F, Morrison SN. Squamous cell carcinoma arising in residual odontogenic cyst. Report of a case and review of literature. *Oral Surg Oral Med Oral Pathol.* 1991;72:218–21. [https://doi.org/10.1016/0030-4220\(91\)90167-b](https://doi.org/10.1016/0030-4220(91)90167-b).

Publisher's Note Springer Nature remains neutral with regard to jurisdictional claims in published maps and institutional affiliations.

Springer Nature or its licensor (e.g. a society or other partner) holds exclusive rights to this article under a publishing agreement with the author(s) or other rightsholder(s); author self-archiving of the accepted manuscript version of this article is solely governed by the terms of such publishing agreement and applicable law.